Biophysical Chemistry 139 (2009) 106–115

Contents lists available at ScienceDirect

Biophysical Chemistry

journal homepage: http://www.elsevier.com/locate/biophyschem

Structural and thermodynamic studies of Bergerac-SH3 chimeras

Liubov' V. Gushchina [a], Azat G. Gabdulkhakov [a], Stanislav V. Nikonov [a], Pedro L. Mateo [b], Vladimir V. Filimonov [a,*]

[a] Institute of Protein Research of the Russian Academy of Sciences, Pushchino, Russia
[b] Department of Physical Chemistry and Institute of Biotechnology, Faculty of Sciences, University of Granada, Spain

ARTICLE INFO

Article history:
Received 5 August 2008
Received in revised form 24 October 2008
Accepted 24 October 2008
Available online 9 November 2008

Keywords:
SH3 domain
β-hairpin stability
Folding thermodynamics
Protein structure

ABSTRACT

Bergerac-type chimeras of spectrin SH3 were designed by extending a β-hairpin by eight amino acids so that the extension protruded from the domain body like a "nose" being exposed to the solvent. A calorimetric study of several Bergerac-SH3 variants was carried out over a wide range of pH values and protein concentrations and the three-dimensional structure of one of them, SHH, was determined. X-ray studies confirmed that the nose had a well defined β-structure whilst the chimera formed a stable tetramer within the crystal unit because of four tightly packed noses. In the pH range of 4–7 the heat-induced unfolding of some chimeras was complex and concentration dependent, whilst at pH values below 3.5, low protein concentrations of all the chimeras studied, including SHH, seemed to obey a monomolecular two-state unfolding model. The best set of data was obtained for the SHA variant, the unfolding heat effects of which were systematically higher than those of the WT protein (about 16.4 kJ/mol at 323 K), which may be close to the upper limit of the enthalpy gain due to 10 residue β-hairpin folding. At the same time, the chimeras with high nose stability, which, like SHH, have a hydrophobic (IVY) cluster on their surface, showed a lower apparent unfolding heat effect, much closer to that of the WT protein. The possible reasons for this difference are discussed.

1. Introduction

The thermodynamic approach to understanding protein folding has reached a point at which the main contributions can be quantified but the accuracy of this quantification is not sufficient for a precise prediction of protein structure. Given the extreme complexity of the problem, further attempts to create simplified models for thermodynamic studies must be welcomed. Since secondary-structure formation is simpler in comparison to protein globule folding, the most valuable thermodynamic information has been obtained from model oligopeptide studies, among which investigation into the helix-coil transition has been most informative [1–6]. The situation with models forming β-structure is much more complicated, first of all due to the well known tendency of the β-structure to make aggregates, very often uncontrollably.

Both experimental and theoretical studies undertaken by several research groups into thermodynamic propensities to form a secondary structure have resulted in the prediction of relatively short sequences to form the most stable β-hairpins and the design of corresponding oligopeptides [7–9]. Several experimental studies into the thermodynamics of β-hairpin unfolding have been published more recently [10–12], but, as far as we know, a direct calorimetric approach has not yet been used for the simple reason that secondary-structure unfolding within relatively short oligopeptides is accompanied by a small heat effect and therefore the temperature-induced transitions are very wide and small in amplitude. This imposes strong demands on the scanning microcalorimeter, which at present are difficult to comply with whilst working at reasonably low peptide concentrations to avoid aggregation.

One possible solution involves inserting a quasi-isolated hairpin into a small globular protein so that it forms a new cooperative unit with the host, which will stabilize the hairpin by fixing its ends. The host must be relatively small so that the contribution of the inserted hairpin to the overall heat effect of unfolding is noticeable. At the same time the whole chimera must be large enough for the overall unfolding heat effect to be measured accurately by DSC. This will only work, however, if the inserted structure unfolds cooperatively with the rest of the molecule. The chimeras made by Serrano's group on SH3 domains, known as "Bergeracs", suit each of these requirements completely [13]. These researchers replaced the N47D48 β-turn of spectrin SH3 by decapeptides with various primary structures, in such a way that the extended β-hairpin protruded from the domain globule like Cyrano de Bergerac's nose and was completely exposed to the solvent. The main idea behind this design was to study the influence of the enlargement of the folding nucleus on kinetic parameters. Unexpectedly, it was found that, unlike the parent

Abbreviations: DSC, differential scanning calorimetry; SH3, Src homology 3 domain.

* Corresponding author. Institute of Protein Research of the RAS, Pushchino, Moscow Region, 142290 Russia. Tel./fax: +7 495 6327871.
E-mail address: vladimir@vega.protres.ru (V.V. Filimonov).

0301-4622/$ – see front matter © 2008 Elsevier B.V. All rights reserved.
doi:10.1016/j.bpc.2008.10.011

domain, some of the Bergeracs with the most stable nose structure folded via a compact intermediate (the so-called "frustration" effect). It remains unknown, however, whether an intermediate state could also be populated under equilibrium conditions and if so, what its structural characteristics might be.

Some data obtained by Viguera and Serrano [13] show that changes in the stability of the protruding β-hairpin modulate the stability of the whole chimera, although the enthalpic and entropic contributions to the Gibbs energy are unknown. If the structure of the nose were stable enough, with a highly co-operative temperature-induced unfolding, DSC would be the most appropriate technique to obtain its thermodynamic functions. Such chimeras would also offer an important advantage in that their folded conformations might be checked quite easily by the conventional methods of structure determination.

We chose five variants of Bergerac-SH3 for calorimetric and structural studies (Table 1). Our selection was based upon results described elsewhere [13] and made with a hairpin thermodynamic and structural investigation in mind.

2. Experimental

2.1. Protein purification

The plasmids bearing the SHH, SHI, SHA, SHT and SHE genes [13] were given to us by Dr. A. R. Viguera. The proteins were expressed and purified as described elsewhere [14]. After checking their purity by SDS electrophoresis the samples were dialysed against 1 mM ammonium carbonate and freeze-dried.

2.2. X-ray analysis

Protein crystals were grown at 22 °C using the hanging-drop vapor-diffusion technique. Several crystal forms were obtained under various conditions but the best quality crystals were grown when 50 mM glycine and 15% sodium malonate (pH 4.5) were used as crystallization reagent. A lyophilised protein sample was dissolved at a concentration of 14 mg/ml in a buffer containing 20 mM sodium acetate and dialysed against this buffer overnight. A 2 μL droplet of protein solution was put onto a cover glass and mixed with another 2 μL of anti-solvent to make the final protein concentration of 7 mg/ml in 7.5% malonate. Under these conditions the crystals reached their maximum size of about 0.8×0.4×0.4 mm^3 within 3 to 4 days. The crystals selected for X-ray studies were transferred into a 20% solution of sodium malonate before freezing.

The data set (Table 2) was collected on a DESY beam line X12 using λ = 1.072 Å radiation equipped with a MAR CCD detector integrated and scaled with XDS [15]. The structure of the Bergerac-SHH chimera was resolved by the molecular replacement method with the MOLREP program [16] using the structure of the D48G mutant of spectrin SH3 ([17]; PDB entry 1BK2) as a search model. Model rebuilding and refinement were undertaken using COOT [18] and REFMAC5 [19] respectively.

Table 1
Fragments of amino-acid sequences of the Bergerac chimeras studied

	1		46abcd 48abcd49		62(70)
WT :	MDE	..	WWKVEV----*ND*----RQG	..	KLD
D48G:	MDE	..	WWKVEV----*NG*----RQG	..	KLD
SHH :	MDE	..	WWKVEV<u>KITV</u>*NG*<u>KTYE</u>RQG	..	KLD
SHI :	MDE	..	WWKVEV<u>KATV</u>*NG*<u>KTYE</u>RQG	..	KLD
SHA :	MDE	..	WWKVEV<u>KATA</u>*NG*<u>KTYE</u>RQG	..	KLD
SHE :	MDE	..	WWKVEV<u>KATA</u>***A***<u>GKTYE</u>RQG	..	KLD
SHT :	MDE	..	WWKVEV<u>KIA</u>V*NG*<u>KAYE</u>RQG	..	KLD

The insertions of 8 amino acids forming the nose are underlined. Two amino acids forming the β-turn are shown in italics. The alanines replacing various positions in SHH are shown in bold type.

Table 2
Crystallographic data collection and refinement statistics

Data collection	
Space group	$P2_12_12_1$
Unit cell parameters (Å, °)	a=49.47, b=57.55, c=101.39, α=β=γ=90.
Resolution (Å) (high-resolution shell)	20.0–1.9 (1.95–1.90)
Redundancy	7.6 (2.3)
Completeness (%)	95.0 (83.1)
R_{merge} (%)	8.1 (41.5)
$I/\delta(I)$	14.93 (2.11)
Refinement statistics	
Resolution range (Å)	20.0–1.9 (1.95–1.90)
No. of reflections	21425 (1511)
Rcryst/Rfree (%)	21.3/26.4
R.m.s.d. bonds (Å)	0.015
R.m.s.d. angles (deg)	1.535
Ramachandran plot analysis (%)	
Most favored	95.3
Additionally allowed	4.7
Generously allowed	0.0
Disallowed	0.0

The final variant of the structure is deposited in PDB under the code 2OAW.

The exposed surface areas were calculated using the Surface Racer program, generously provided by Dr. O. Tsodikov [20].

2.3. Differential scanning calorimetry (DSC)

The temperature dependencies of the partial heat capacity for chimeric proteins were obtained using a SCAL-1 microcalorimeter [21] with a cell volume of 0.32 ml at a heating rate of 1 K/min. The lyophilised protein samples were dissolved in an appropriate buffer and dialysed overnight with two changes of dialysis solution. Protein concentration was measured spectrophotometrically at 280 nm using the following molar extinction coefficients: 16150 cm^{-1} M^{-1} for the WT protein and its D48G mutant, and 17300 cm^{-1} M^{-1} for all the Bergerac chimeras. The thermodynamic parameters of protein unfolding were calculated either from a single- or multiple-curve fitting of $C_p(T)$ functions presented as

$$C_p(T) = C_p^{exc}(T) + C_p^{int}(T) \quad (1)$$

by procedures described elsewhere [22]. The equations for the monomolecular two-state model are

$$\Delta_N^U C_p(T) = C_{p,U}(T) - C_{p,N}(T) \quad (2)$$

$$C_p^{int}(T) = C_{p,N}(T) + F_U(T)\Delta_N^U C_p(T) \quad (3)$$

$$C_p^{exc}(T) = \frac{(\Delta_N^U H)^2 F_U F_N}{(2-F_U)RT^2} \quad (4)$$

where $C_{p,U}(T)$ and $C_{p,N}(T)$, and F_U and F_N are the heat capacities and fractions of the native and unfolded states correspondingly, and were used for curve-fitting assuming linear approximations for the $C_{p,N}(T)$, $C_{p,U}(T)$ and $\Delta_N^U C_p(T)$ functions. The four-state monomolecular scheme was used for C_p^{exc} curve simulations [23] as described in the text.

2.4. Fluorescence spectroscopy and urea-induced unfolding

The fluorescence spectra were recorded in the wavelength range of 300–500 nm using a Shimadzu RF-5301 PC spectrofluorimeter with a

1 cm cell at urea concentrations in the range of 0–9 M and a constant SHA concentration of 5 μM. The excitation wavelength was 293 nm and exact urea concentration was measured by refraction index as described in [24]. The "center of mass" of each spectrum was calculated as described in [25] using the formula

$$\lambda_{CW} = \frac{\sum_{i=1}^{n} \lambda_i I_i}{\sum_{i=1}^{n} I_i} \quad (5)$$

where I_i was spectrum intensity at wavelength λ_i. The λ_{CW} points were plotted against urea concentration and fitted to the modified linear extrapolation two-state model (BEM) as described in [24].

3. Results

3.1. Three-dimensional structure

The most stable SHH variant with a "frustrated" refolding kinetic was chosen as the best candidate for X-ray studies. The crystals were grown at pH 4.5 and under these conditions this chimeric protein formed tetramers within the crystal cell (Fig. 1). We found that four nose tips were responsible for tetramerisation whilst domain bodies practically did not interact with each other within the elementary unit. A more detailed analysis of the nose area (Fig. 2) revealed that the clusters formed by the I46b/V46d/Y48c side-chains (IVY cluster) of each beta-hairpin made a well packed hydrophobic core. According to the Surface Racer program there were no big cavities within this core, so it is was as tightly packed as any hydrophobic core of a small globular protein. A network of the intra- and inter-chain hydrogen bonds should also help to stabilize this conformation. As can be seen in Fig. 3, the main part of the SHH chain follows closely the conformation of the D48G mutant with the exception of the positions flanking the insert and forming the RT-loop (res. 19–21). Both anomalies are probably caused by crystallization effects: a careful analysis of the SHH X-ray data reveals notable differences in nose orientation with respect to the domain body between the four chains packed into the crystal cell (Fig. 3). It would seem that the high RMSD values for the nose region are caused by a deflection

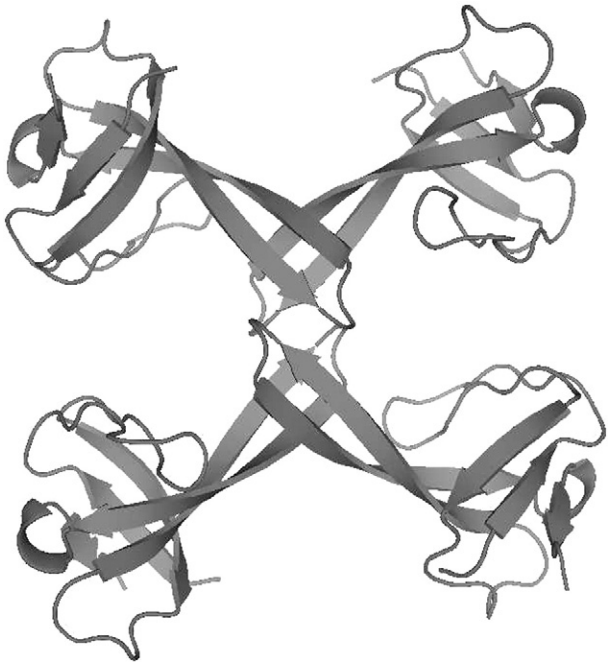

Fig. 1. The cartoon model of the SHH tetramer forming the crystal unit. Four "noses" make a well-packed complex in the center.

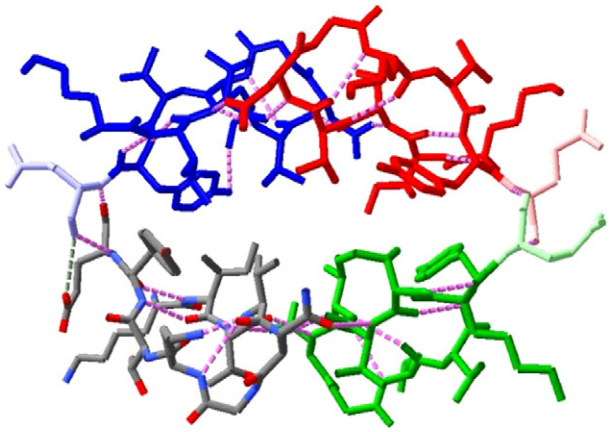

Fig. 2. The fragment of the SHH tetramer structure showing the complex of four "noses" (KITV*N*GKTYE sequences, each marked by a different color). The hydrogen bonds are shown as pink dashed lines; C-terminal glutamic-acid residues are shown in light colors. (For interpretation of the references to colour in this figure legend, the reader is referred to the web version of this article.)

of the β-hairpins from relaxed positions in their tendency to form a tight tetramer within the crystal. Similarly the flexible RT-loop is fixed in a distorted conformation due to a steric clash between the side chains of R21 belonging to adjacent crystal cells.

The conformation of the NG beta-turn in D48G-SH3 differs slightly from that of SHH: it is more tightly packed and the angles in the Ramachandran plot are also slightly different. We also studied the structures of the SHA and SHH variants by NMR [26]. According to our observations, the polypeptide chain conformations of SHH and SHA coincide closely, although the RMSD values are somewhat higher for the nose region. Nevertheless, in solution the inserts always adopt the β-hairpin conformation, with all hydrogen bonds properly formed. At pH 3.0, however, the NMR spectra do not reveal any tendency either in SHA or in SHH to form tetramers even at the high protein concentrations (about 1 mM) used in our studies.

3.2. Two-state unfolding studied by DSC

In a previous study it was found that many Bergeracs obeyed a two-state folding kinetic, but the most stable SHH chimera and a couple of

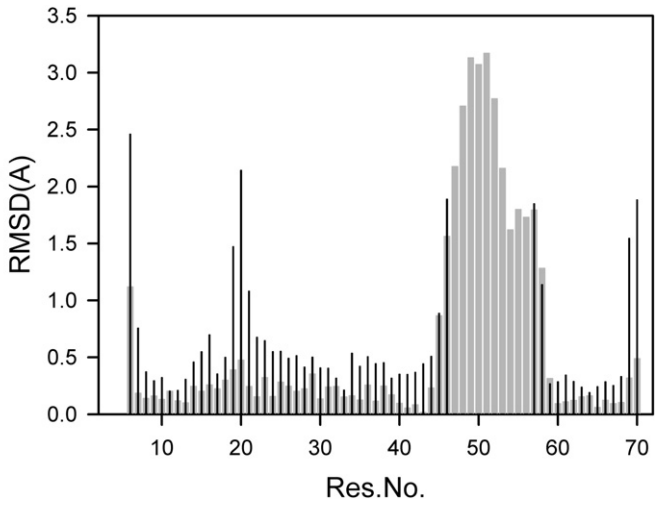

Fig. 3. The root mean square deviations (RMSD) between the backbone atoms of two homologous structures (grey bars indicate deviations between chains A and B in the SHH crystal cell, and black bars deviations between the homologous fragments of the D48G-SH3 mutant and chain A of SHH). The structures were superimposed using the SpdbV program. Residue numbering corresponds to the polypeptide chain of SHH.

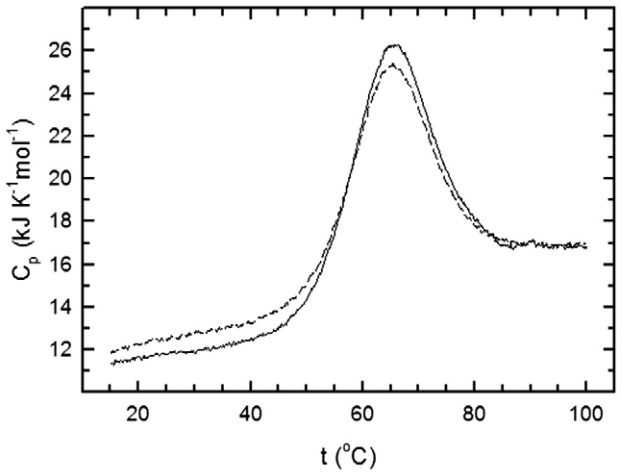

Fig. 4. DSC curves for SHH at pH2.9 and protein concentration 220 μM. Solid line, first heating; dashed line, reheating of the same sample.

other variants had non-ideal chevron plots with somewhat curved refolding wings [13,27]. Therefore we deemed it interesting to study here, under equilibrium conditions, whether the addition of the nose in the chimeras might also increase the population of unfolding-equilibrium intermediate state(s), as manifested in the $C_p(T)$ curves. Two variants, SHI and SHA, differed from SHH by single and double replacements of the massive hydrophobic groups of the IVY cluster by alanine (Table 1), which, according to the urea-induced unfolding data, not only resulted in decreased stability in their structure compared to SHH but also exhibited almost ideal chevron plots. Another interesting variant, SHE, has a N/A replacement within the optimized beta-turn. To some extent this latter variant was an analogue of the N47A-SH3 mutant, which showed a very strong and unexpected tendency to form oligomers and amyloids under quite mild conditions [28].

At pH 7.0 the heat-induced unfolded states of all the Bergeracs showed quite a strong tendency to form oligomers and/or large aggregates. This behaviour is typical of most globular proteins close to the isoelectric point. Nevertheless, in the pH range 2.5–3.5, at reasonably low protein concentrations (below 250 μM) and low ionic strength (25 mM), the heat-induced unfolding of all the variants was highly reversible (Fig. 4), whilst the heat-absorbance profiles did not depend either upon heating rate or protein concentration. Most of the $C_p(T)$ functions recorded under these conditions fit very well to the simple two-state model, either each curve separately (Fig. 5) or as a curve family simultaneously (Fig. 6). The quality of fitting is fairly high

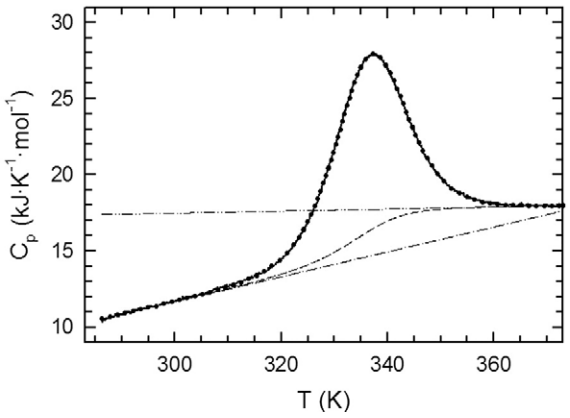

Fig. 5. Temperature dependence of the molar heat capacity of the SHE variant at pH = 3.0 and protein concentration of 220 μM (solid line) and its best fitting to the two-state model (dots). The best fitting $C_{p,N}$ (dash-dot line), $C_{p,U}$ (dash-dot-dot line) and C_p^{int} (dashed line) are also shown.

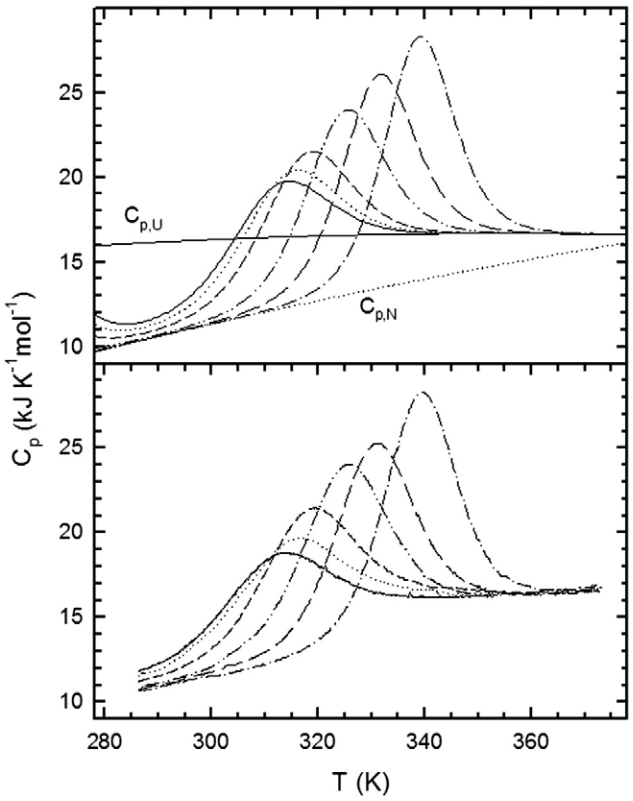

Fig. 6. Temperature dependencies of the partial molar heat capacity for SHA at various pH values: 2.0 (___); 2.2 (....); 2.5 (- - -); 2.8 (_.._); 3.0 (_) and 3.5 (_._._). Lower panel: experimental data at protein concentrations of about 250 μM; upper panel: the curves simulated using Eqs. (7)–(9) and the data from Table 3.

and does not imply that other states except for the native and unfolded ones are populated.

The unfolding behavior of the SHA variant was the best under all conditions and it was possible to reduce its unfolding midpoint, T_m, ($\Delta_N^U G(T_m)=0$) down to room temperature simply by changing pH. Consequently we have set out the data relevant to this variant in Fig. 6. According to DSC data, the dependence of SHA's structural stability upon pH closely follows that of the WT protein above pH 3.0 (Fig. 7), whilst below this value the T_m(pH) curve is shallower, indicating that the nose insertion results in additional pK shifts of some acidic groups. The most probable candidates for these shifts are E45 and E48d (nose),

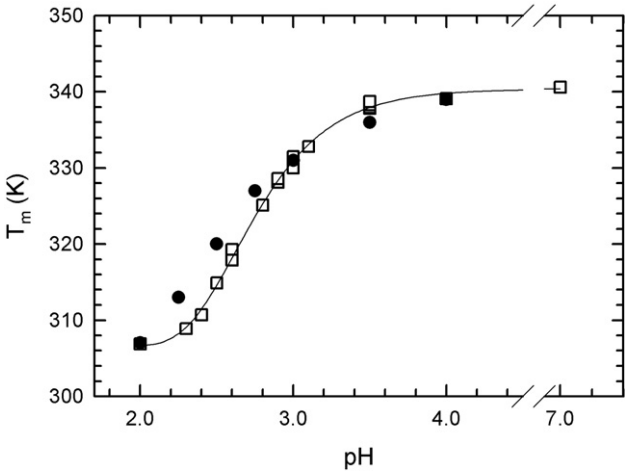

Fig. 7. The dependencies of the transition midpoint, T_m, upon pH for SHA (open squares) and the WT protein (filled circles) [14,29]. The solid line shows a best-fit sigmoid drawn through the SHA data.

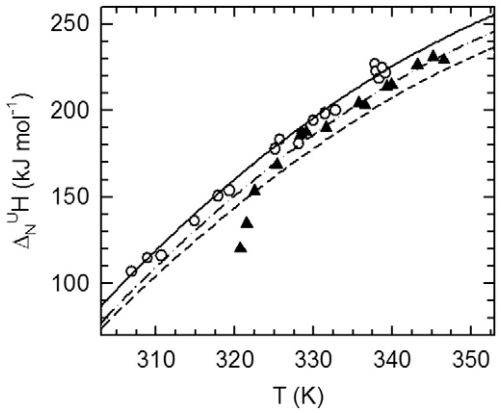

Fig. 8. Correlations between the unfolding heat effect and temperature for SHH (solid triangles) and SHA (open circles). The dashed line corresponds to Eq. (6) deduced for the WT family in [29]. The solid and dashed-dotted lines represent Eqs. (9) and (10) respectively.

the carboxylic groups of which within the SHH structure are in close proximity to the amino group of K46a (see residue numbering in Table 1). In any case, the changes in the dependence of T_m(pH) should be entropic as the protonation heats for the carboxylic groups are close to zero. Apart from that, since this triad is present in all the Bergeracs studied one might expect that the pH dependencies of T_m for other Bergeracs have similar shapes, although displaced vertically according to the changes in their stability (the displacements at pH 3.0 are shown in Table 4). As far as the unfolding heat effects are concerned, in previous studies into single and multiple mutants of spectrin SH3 [29] the empirical dependence of the unfolding enthalpy upon temperature for the WT family was expressed as

$$\Delta_N^U H(T) = 5.13 \cdot (T - T_h) - 0.019 \cdot (T - T_h)^2 - 6 \cdot 10^{-5} \cdot (T - T_h)^3 \quad (6)$$

where T_h=287.6 K ($\Delta_N^U H(T_h)$=0). The following empirical relations were deduced for SHA from an analysis of the DSC data shown in Figs. 6 and 8 and $C_{p,U}$ approximations made according to the procedure of Makhatadze and Privalov [30]:

$$C_{p,U}(T) = 17.06 + 0.032 \cdot T - 1.785 \cdot 10^{-4} \cdot T^2 \quad (7)$$

$$\Delta_N^U C_p(T) = 5.77 - 0.116 \cdot (T - T_h) \quad (8)$$

$$\Delta_N^U H(T) = 5.77 \cdot (T - T_h) - 0.058 \cdot (T - T_h)^2 \quad (9)$$

where T_h=286.6 K.

The temperature dependencies of unfolding heat effects for other Bergeracs (SHH, SHI, SHE and SHT) in the pH range 2.5–3.5 can be approximated by the empirical relation

$$\Delta_N^U H(T) = 5.674 \cdot (T - T_h) - 0.058 \cdot (T - T_h)^2 \quad (10)$$

where T_h=288.3 K (dashed-dotted line in Fig. 8).

From these relations and Fig. 8 it can be seen that the temperature dependence of the unfolding enthalpy for SHA lies higher than that of the WT family whilst the data for other variants lie between these two lines. The difference between the WT and SHA enthalpy functions, $\delta\Delta_N^U H(T)$, which exceeds the experimental error, appears to be temperature dependent and therefore it seems reasonable to choose some average temperature to provide an estimate. Taking 323 K as a reference temperature, we get 16.4±4 kJ/mol for $\delta\Delta_N^U H$, whilst the unfolding heat effect of SHA exceeds that of other variants by about 10 kJ/mol.

DSC data (Tables 3 and 4) also confirm the differences in stability between the Bergeracs reported elsewhere [13]. Nevertheless, the thermal stability expressed as apparent T_m values has to be transformed into $\Delta_N^U G^0$ values to be compared with the same parameter measured in urea-unfolding experiments. This is a long extrapolation and depends very much upon the accuracy of the determination of $\Delta_N^U C_p(T)$. Since the main difference in unfolding behaviour is between SHH and SHA, we set out in Table 3 the DSC results for WT protein and these two most thoroughly studied Bergeracs together with the data on urea-induced unfolding of SHA. An obvious discrepancy between some parameters of heat- and urea-induced melting will be discussed below.

The higher slopes of $\Delta_N^U H(T)$ for SHA and SHH compared to the WT family proteins indicate that the apparent $\Delta_N^U C_p$ for the Bergeracs is also somewhat higher. Unfortunately the accuracy of a direct determination of $\Delta_N^U C_p$ from the wide DSC curves is rather low (about 20%), which precludes any direct comparison between the observed $\Delta_N^U C_p$ and the slope of $\Delta_N^U H(T)$. Nevertheless, $\Delta_N^U C_p$ could be estimated from structural data using the empirical algorithms suggested by several groups. With the exception of a few alternative points of view [31] it is generally accepted that the increase in heat capacity upon unfolding is proportional to a linear combination of the hydrophobic and hydrophilic areas exposed upon unfolding [32], although more complicated algorithms based on exposed-area calculations have also been suggested [24,33–35]. The establishment of more exact correlations is hampered by uncertainties both in the thermodynamic and structural data, the greatest uncertainty deriving from the choice of a structural model for the unfolded state. Currently the extended beta-structure is accepted as being the best approximation, although it is well known that fluctuating alpha or polyproline helices are among the preferred conformations of the unfolded polypeptide chains [36–38]. The structures of the folded states are much better defined, although there might be serious discrepancies between the exposed area calculated from the

Table 3
The thermodynamic parameters of unfolding for the WT protein and two variants of Bergerac-SH3 chimeras

n	pH	T_m (K)				$\Delta_N^U H(T_m)$ (kJ mol^{-1})				$\Delta_N^U G(298)$ (kJ mol^{-1})					*m* (kJ mol^{-1} M^{-1})
		WT	D48G	SHH	SHA	WT	D48G	SHH	SHA	WT	D48G	SHH	SHA		SHA[a]
1	2.0	307.0	318.3	322.5	306.9	93.0	140.0	153.5*	106.9	2.3	6.4	7.7	2.3	–	–
2	2.25	313.0	–	325.3	308.9	114.0	–	168.3*	114.7	4.2	–	9.5	3.5	–	–
3	2.5	320.0	324.6	329.0	314.9	139.0	170.0	187.6	136.3	6.9	9.8	11.3	5.2	2.9	–
4	2.75	327.0	–	335.7	324.8	162.0	–	203.9	177.8	9.8	–	14.7	9.1	6.4	4.3
5	3.0	331.0	333.4	337.9	330.0	174.0	196.0	210.2	194.3	11.6	14.0	16.0	12.8	11.7	3.6
6	3.5	336.0	343.9	345.3	338.3	188.0	214.0	230.6	220.0	13.9	18.3	20.4	16.9	24.4	4.4
7	4.0	339.0	347.2	–	339.1	197.0	225.0	–	237.5	15.6	20.5	–	17.5	24.9	4.7
8	7.0	–	–	–	340.6	–	–	–	–	15.0[a]	–		18.4	19.2	3.9

The heat effects denoted by asterisks were obtained by extrapolation of the dashed-dotted line in Fig. 8. The data for the WT and D48G are taken from Refs. [17] and [29] respectively.
[a] Values taken from urea-induced unfolding.

Table 4
The thermodynamic parameters of Bergerac chimeras unfolding at pH 3.0 (25 mM glycine) calculated from DSC data

	Chimera	T_m (K)	$\Delta_N^U H(T_m)$ (kJ mol^{-1})	$\Delta_N^U S(T_m)$ (kJ K^{-1} mol^{-1})	$\Delta_N^U G(298)$ (kJ mol^{-1})
1	SHH	337.9	210.0	0.621	16.0
2	SHE	333.3	196.6	0.590	13.5
3	SHI	332.1	192.9	0.581	12.9
4	SHT	330.0	186.2	0.564	11.8
5	SHA	330.0	194.3	0.589	12.8

structural data obtained by X-ray crystallography and that obtained by NMR spectroscopy, even for such small, rigid molecules as SH3 domains [24].

The uncertainty in the DSC data on protein unfolding is never less than 5%, whilst in many cases the accuracy of establishing $\Delta_N^U C_p$ is even less precise. In these circumstances the sophisticated ΔASA *vs* ΔC_p correlations deduced from a statistical analysis of the data available are useless. Nevertheless, we tried to estimate $\Delta_N^U C_p$ from the structural information available for SHH, SHI and SHA using the simplest [34] and most elaborate [35] algorithms (see Table 5). It should be noted here that we are taking this structural information to be similar to that corresponding to the folded state in solution, for which different conformations could in fact coexist given the certain flexibility of the beta-turn. We are assuming then that our structural data (and its energy contribution to the folded state) are close enough to that of the average of the possible conformations in solution.

The calculations (Table 5) predicted a small increase in $\Delta_N^U C_p$ for the Bergeracs compared to the WT variant, which qualitatively agrees with the data contained in Fig. 8.

3.3. Urea-induced unfolding of SHA

The published thermodynamic data on urea unfolding of Bergeracs were obtained from kinetic studies at two pH values, 7.0 and 3.0 [13]. To extend this data set we have undertaken equilibrium studies into urea unfolding of SHA using tryptophan fluorescence as detection technique. The spectra (not shown) were measured at 25 °C as functions of urea concentration for a selection of pH values. Each set of spectra was treated as described in the Experimental section and the resulting unfolding curves are shown in Fig. 9. Whereas $\Delta_N^U G^0$ values calculated for SHA from DSC and urea experiments closely coincide at pH 3.0 (Table 3), there is a large discrepancy between the two sets of data at higher pH values. It is noteworthy that not only the $\Delta_N^U G^0$ values obtained by extrapolation but

Table 5
The exposed areas calculated for several variants of spectrin SH3 together with the $\Delta_N^U C_p$ and ***m*** values estimated from these areas

		WT (1SHG)	D48G (1BK2)	SHH (2OAW)	SHI	SHA
Total ASA, Å^2	Folded	3919.22	3801.77	4687.58	4669.28	4662.04
	Beta strand	8513.25	8521.77	9645.27	9605.78	9583.68
	ΔASA	4594.03	4720.0	4957.69	4936.5	4921.64
Polar ASA, Å^2	Folded	1812.03	1764.28	2152.38	2158.42	2172.72
	Beta strand	3631.73	3555.07	4048.71	4060.57	4070.62
	ΔASA	1819.70	1790.79	1896.33	1902.15	1897.9
Apolar ASA, Å^2	Folded	2107.19	2037.49	2535.20	2510.86	2489.32
	Beta strand	4881.52	4966.71	5596.57	5545.20	5513.06
	ΔASA	2774.33	2929.21	3061.37	3034.34	3023.74
$\Delta_N^U C_p$, kJ K^{-1} mol^{-1}	Ref. [34]	3.65	3.75	3.94	3.92	3.91
	Ref. [35], 298 K	3.08	3.40	3.52	3.46	3.45
	Ref. [35], 323 K	2.80	3.09	3.21	3.15	3.14
m, kJ mol^{-1} M^{-1}	Ref. [34]	2.7	2.8	2.9	2.9	2.9

The names of the SH3 variants are given in column headers together with corresponding PDB entries. The calculations for the SHI and SHA variants were made after introducing corresponding mutations into the SHH structure using SpdbV Program. The algorithms from indicated references were used for estimating $\Delta_N^U C_p$ and ***m*** values.

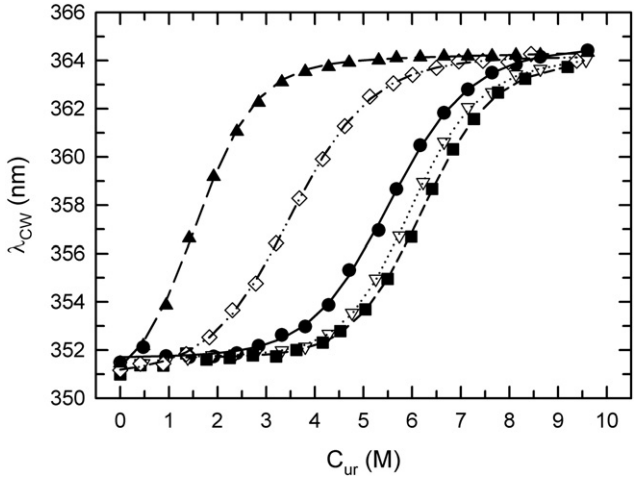

Fig. 9. Dependencies of the centers of weight, λ_{CW}, of the fluorescence spectra upon urea concentration for SHA at various pH values: filled circles, pH7.0; open triangles, pH 4.0; filled squares, pH 3.5; open squares, pH 3.0 and filled triangles, pH 2.8. The lines show the best fittings to the BEM two-state model.

also the *m* and $C_{ur,\ 1/2}$ parameters are unexpectedly higher than the corresponding ones for the WT protein. Besides this, to our surprise the structure of SHA seems to be more stable against urea-induced unfolding at pH 4 and 3.5 than at pH 7.0. This behavior is totally different from that of the WT and some of its mutants [14,24,39,40], which show a uniform dependence of their stability upon pH, whether the unfolding is induced by temperature or by urea.

3.4. Non-two-state behaviour

Above pH 4.0, or even below it at relatively high protein concentrations, the DSC curves of some variants (SHH, SHI and SHE) became more complicated. The clearest deviations from the two-state behaviour were observed for SHH. As can be seen in Fig. 10, at pH 4.0 the heat-capacity profiles became concentration dependent, showing two peaks even at modest protein concentrations. Concentration dependence is such that one peak moves to the left and the other to the right, which means that the intermediate state must have a higher state of oligomerization than the native and unfolded ones. Whilst SDS electrophoresis always proved the high chemical homogeneity of the Bergerac samples, electrophoresis under native conditions (i.e. without detergent) at pH 4 sometimes showed the presence of species

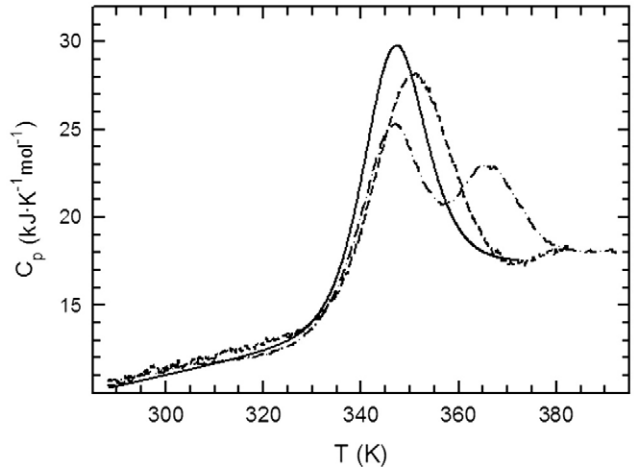

Fig. 10. Temperature dependencies of the SHH heat capacity in 25 mM sodium acetate (pH 4.0) at high (318 μM, dashed-dotted line) and low (146 μM, dashed line) protein concentrations. For comparison the melting curve recorded at pH 3.5 is shown as a solid line.

that moved more slowly than the monomer. DSC data do not clearly indicate, however, that the native state forms oligomers at moderate concentrations.

Unfortunately, the properties of this two-peak curve are not easily reproducible and cannot be unambiguously interpreted within the simple equilibrium three-state model

$$N \rightleftharpoons \frac{1}{n} I_n \rightleftharpoons U \tag{11}$$

where I_n is an intermediate oligomer, as is the case with the unfolding of the Cro-repressor [41]. In general the situation seems to be so complicated that as yet we cannot offer a precise interpretation of all the non-two-state curves.

At the same time, pH values below 2.5 also produced strange though less spectacular effects on the melting curves of SHH and, to some extent, of SHE. Although the curves recorded at pH 2.5 and below fitted the two-state model, the heat effect calculated by curve fitting dropped well below the $\Delta^U_N H(T_m)$ correlation for the WT protein (Fig. 8). Since no traces of chain degradation of concentration dependence were detected, this strange behaviour must be put down to a combination of factors, most probably a complex pH-dependence of the stability of all the states populated during the unfolding of chimeras bearing the IVY cluster.

4. Discussion

The results presented above delineate a rather complex pattern, which, depending upon experimental conditions, might be conventionally divided into three parts:

1) the apparent two-state unfolding of all Bergeracs in the pH range 2.5–3.0 (extendable up to pH 4.0 in the case of the heat-induced unfolding of SHA) with a negligible population of intermediate states;
2) the non-two-state behavior in the pH range 3.5–7.0 with the unusual influence of urea on unfolding transitions;
3) the complex behavior of SHH below pH 2.5, where the folded conformations of other Bergeracs are only marginally stable.

The most important for thermodynamic considerations is the first set of data, which contains no contradiction between the results of heat- and urea-induced unfolding. According to the data from the DSC study the cooperative SHA melting is accompanied by an additional heat effect that may be put down to a great extent to the average unfolding energy of the nose conformation(s). It would then be tempting to attribute all that heat effect (about 16 kJ/mol at 323 K) to the break down of the additional hydrogen bonds formed within the β-hairpin, as well as to other factors such as van der Waals interactions, hydrophobic and hydrophilic effects that might also have significant enthalpy terms [4,42–44], although the mere fact that $\delta\Delta^U_N H$ is temperature dependent implies hydrophobic and hydrophilic contributions to the unfolding heat. The changes in Gibbs energy calculated for SHA from DSC and urea data at pH 3.0 coincide, which also speaks in favor of a two-state unfolding under these conditions.

A careful inspection of the $\Delta^U_N H(T_m)$ plots calculated from the DSC data for other Bergerac variants using the two-state model shows that most of them have a lower unfolding heat effect than that of SHA, which seems a bit strange in view of their higher stability. Even assuming the average nose conformations of SHH, SHI and SHA to be equal, several possible reasons for these differences might apply. They may well be natural in origin, such as differences in nose–solvent interactions due to different sizes of the hydrophobic cluster formed on the nose surface by residues 46b,46d and 48c (the IVY cluster in SHH), or else they may also reflect some limitations in the data analysis algorithms. For example, the unfolding behaviour of the most stable Bergeracs might significantly deviate from the monomolecular two-state model, thus resulting in a systematic error of enthalpy evaluation from the DSC curves.

As to the former possibility, it has been shown recently that the side chains can be divided into three groups with respect to their contribution to the overall heat effect of α-helix formation [4]. Among other factors, there is a clear difference between β-branched residues and alanine. The replacement of alanine in an α-helix by valine or isoleucine will reduce the heat effect of folding by approximately 1 kJ/mol. It is not completely clear whether a similar heat effect occurs when branched residues are replaced by alanine in β-hairpins, but if it were of the same order of magnitude then the replacement of both valine and isoleucine in SHH by two alanines in SHA would increase the heat effect of nose unfolding by about 2–3 kJ/mol, which is far lower than the observed difference. Nevertheless, this effect should be taken into account when further experiments are planned.

In order to clarify how the stability of the residual structure could influence our DSC results we tried to simulate the unfolding behavior of Bergerac chimeras by using a simple two-block (four-state) model [23,45]. Let us assume that the isolated average nose conformation might be folded and its unfolding, as well as the unfolding of an isolated domain, obeys the two-state model. Then any Bergerac polypeptide chain may populate four macroscopic states, as shown in Fig. 11. The equilibrium constants corresponding to the unfolding of the same unit are not necessarily equal if the stability of one region depends upon the state of another, although the equilibrium constant for the transition between states *N* and *D*

$$K_{ND} = K_{D1} \cdot K_{N2} = K_{D2} \cdot K_{N1} \tag{12}$$

does not depend upon the unfolding pathway. Thus, if the native state is taken as a reference, the partition function *Q*, which defines the fractions of all states as

$$F_{Df-Nf} = \frac{1}{Q}; \quad F_{Du-Nf} = \frac{K_{D1}}{Q}; \quad F_{Df-Nu} = \frac{K_{N1}}{Q}; \quad F_{Du-Nu} = \frac{K_{ND}}{Q} \tag{13–16}$$

can be written as

$$Q = 1 + K_{D1} + K_{N1} + K_{ND} \tag{17}$$

Using these equations the $C_p^{exc}(T)$ function is easily expressed through the enthalpy and entropy changes for individual transitions.

To further simplify the model we assumed that the heat effects of unfolding do not depend upon the state of the partner, i.e. the difference between K_{D1} and K_{D2} (K_{N1} and K_{N2}) is due to entropic terms (different T_s values, $\Delta^Y_X S(T_s)=0$). Using the data accumulated for isolated beta-hair-

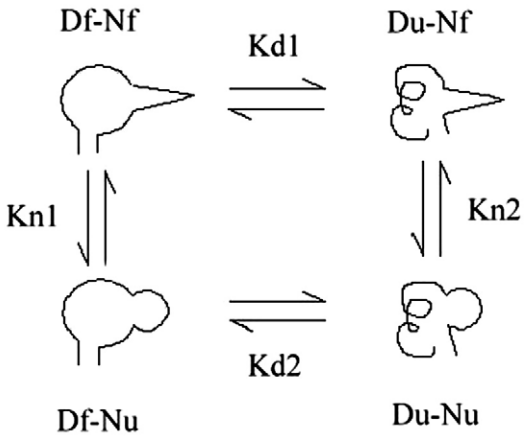

Fig. 11. The equilibrium unfolding scheme for a molecule consisting of two cooperative units: D (domain) and N (nose). Each unit might be in a folded (f) or unfolded (u) state and unfold first (1) or second (2).

pins and the spectrin SH3 domain we can estimate the thermodynamic parameters (in particular the enthalpy change) for the transitions N_1 and D_2. As a starting point it is quite natural to assume that the Gibbs energy change of the N_2 transition is somewhat lower than 0 because the fraction of the folded, isolated nose is about 30% at 298 K [13]. For practical purposes the temperature dependence of the unfolding heat effect for the WT and D48G can be represented approximately by a quadratic function

$$\Delta_N^U H(T) = a + b \cdot T + c \cdot T^2 \quad (18)$$

which results in

$$\Delta_N^U C_p(T) = 21.1 - 0.0547 \cdot T \quad (19)$$

These two functions were used for simulations of the unfolding parameters of the domain block, i.e. for transitions D_1 and D_2 within the chimeras. The T_h/T_s variant of expressing ΔH and ΔS was chosen since $\Delta G_{D2}(T)$ might be well below 0, even for SHH, which means that T_m cannot exist. Assuming for simplicity's sake that ΔC_p is constant we get, for example,

$$\Delta H_{N2}(T) = \Delta C_{p,N2}\left(T - T_{h,N2}\right) \quad (20)$$

$$\Delta S_{N2}(T) = \Delta C_{p,N2} \ln\left(T/T_{h,N2}\right) \quad (21)$$

The results of C_p^{exp} curve simulations and their analysis according to the two-state model appear in Fig. 12 and Table 6. The parameters for the simulations were chosen empirically with some simplifications. For example, it was assumed that the amino-acid replacements only influence the entropic contribution to the stability of the nose. The main criterion was to achieve the close correspondence of the simulated excess heat-absorbance functions, $C_p^{exp}(T)$, with those found experimentally. Although the scheme looks rather simplistic, the parameters of four transitions look quite reasonable for both SHH and SHA. One technical aspect has to be noted: the DSC curves fit very well to the two-state model even when the population of the folded nose after domain unfolding at high temperatures (SHH) reaches as much as 20% (curves not shown). This is because of the small heat effect of nose unfolding, which results in a low, wide C_p^{exp} peak overlapping the main transition.

According to our simulations SHA should unfold quite cooperatively and the folded nose population should be quite negligible, whereas in the case of SHH the hairpin population at 348 K (well above domain T_m at pH 3.0) may reach as much as 20%, which might

Table 6
Input parameters for simulations in accordance with the equilibrium scheme (Fig. 8, Eqs. (12)–(21)); the calculated free-energy changes and the results of the best fitting of the simulated excess heat-capacity functions to the two-state unfolding model

	SHH	SHH	SHA
	Variant 1	Variant 2	Variant 1
Simulation input			
a, kJ/mol	−3806	−3806	−3806
b, kJ/K mol	21.1	21.1	21.1
c, kJ/K^2 mol	−0.02735	−0.02735	−0.02735
$T_{m,\,D2}$, K	306	306	306
$\Delta C_{p,N2}$, kJ/K ·mol	0.4	0	0.4
$T_{h,N2}$, K	280.0	ΔH_{N2} = const = 18 kJ/mol	280
$T_{s,N2}$, K	260.0	ΔS_{N2} = const = 0.066 kJ/K mol	276
ΔS_{12}, kJ/K ·mol	0.06	0.06	0.06
Simulation results			
ΔG^0_{D2}, kJ/mol	1.87	1.87	1.87
ΔG^0_{N2}, kJ/mol	−1.94	−1.67	−9.06
ΔG^0_{D1}, kJ/mol	19.75	19.75	19.75
ΔG^0_{N1}, kJ/mol	15.94	16.21	8.82
$\Delta_N^U G^0$, *kJ/mol*	17.81	18.08	10.69
$\Delta\Delta G^0_{12}$, kJ/mol	17.88	17.88	17.88
Best fit results			
ΔC_p, kJ/K mol	2.99	3.37	4.7
$T_{m,bf}$, K	338.1	337.7	325.7
$\Delta H_{m,bf}$, kJ/mol	221.7	216.3	183.2

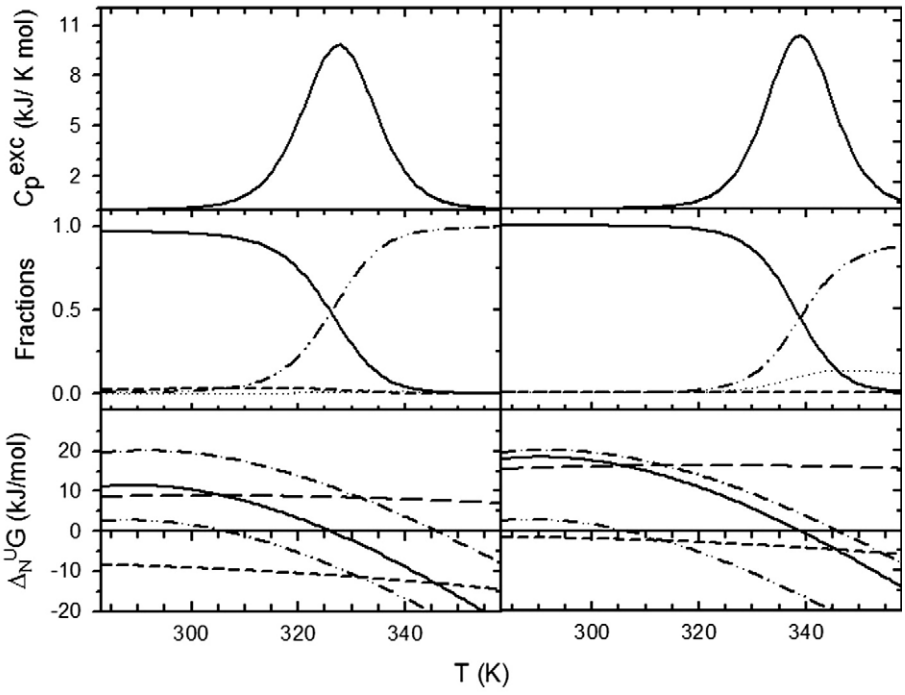

Fig. 12. The results of simulations for Bergeracs unfolding at pH 3.0 using a two-block scheme. Left-hand panels, SHA, right-hand panels, SHH. Upper panels, excess heat capacity and their best fittings to the two-state model (two lines are visually undistinguishable). Middle panels, state fractions: F_{NN}, solid lines; F_{UU}, dash-dot-dot lines; F_{NU}, dashed lines; F_{UN}, dotted lines. Lower panels, Gibbs energy changes for the transitions: short dash, ΔG_{N2}; long dash, ΔG_{N1}; dash-dot-dot, ΔG_{D2}; dash-dot, ΔG_{D1}; solid lines $\Delta_N^U G(T) = \Delta G_{D1} + \Delta G_{N2}$. The input parameters of simulations are show in Table 6 together with the C_p^{exc} fitting results.

result in an underestimation of the apparent unfolding heat effect by curve-fitting procedures by 3–4 kJ/mol. This margin is still smaller than the observed difference between SHA and SHH, which may well suggest that some intermediate state bigger than the folded nose (D_UN_F) but still smaller than the folded domain might be populated under certain conditions. Thus, for example, within the unfolded state the nose can join up with its distal extension to form a long, stable hairpin (11 pairs of residues between D40 and A63), or the nose may stick via its IVY cluster to another hairpin within the same partially unfolded chain, thus making a relatively large misfolded nucleus. The $\Delta_N^U H$ values found for SHT from DSC experiments are closer to those for SHH than for SHA, again indicating that the presence of an IVY cluster may play an important role in the real reduction of the heat effect.

In addition to the stabilization of some monomolecular intermediates caused by the "nose" insertion, another frequent scenario for the β-structured proteins may take place. Spectrin SH3 had the reputation of being a good two-state folder up to the moment when a concentration dependence of its DSC curves was revealed [46]. Later it was found that the single replacement N47A within the distal β-turn resulted in a strong tendency for the polypeptide chain to rapidly form amyloids during heat-induced unfolding [28]. The addition of a new element with a strong β-structural propensity may enhance this tendency, which is supported by SHH behavior in DSC experiments above pH 3.5 and our data on urea-induced unfolding of SHA above pH 3.0. Possible candidates for "alternative" oligomeric conformers formed at moderate pH values and low urea concentration could be dimers or even the tetramers revealed in this study by X-ray analysis of SHH. A sort of intertwined structure like the one reported for the Eps8 SH3 domain would also be feasible [47].

In summary, it would seem that a complex interplay between the propensities to form β-structure and β-turns, modulated by electrostatic interactions and protein concentration, play a very important pH-dependent role in directing the polypeptide chain into β-hairpins or antiparallel interchain β-sheets and subsequent aggregation. Further experiments with a similar nose stuck to another globule with a lower propensity to form long β-hairpins or stable misfolded conformations would shed more light on the situation. Nevertheless, the DSC data obtained in this study for SHA are free from these complications and provide a rather good, direct estimation for the heat effect of its nose hairpin formation.

Acknowledgements

This research was supported by INTAS Grant 03-51-5569, MCB RAS Programme and RFBR Grant 03-04-48331. We thank Dr. A. R. Viguera for his generous gift of the plasmids and Dr. J. Martínez for his helpful advice. We also thank. Dr. J. Trout for revising our English text.

References

[1] R.L. Baldwin, Alpha-helix formation by peptides of defined sequence, Biophys. Chem. 55 (1995) 127–135.
[2] I. Luque, O.L. Mayorga, E. Freire, Structure-based thermodynamic scale of alpha-helix propensities in amino acids, Biochemistry 35 (1996) 13681–13688.
[3] J.K. Myers, C.N. Pace, J.M. Scholtz, A direct comparison of helix propensity in proteins and peptides, Proc. Natl. Acad. Sci. USA 94 (1997) 2833–2837.
[4] J.M. Richardson, M.M. Lopez, G.I. Makhatadze, Enthalpy of helix-coil transition: missing link in rationalizing the thermodynamics of helix-forming propensities of the amino acid residues, Proc. Natl. Acad. Sci. USA 102 (2005) 1413–1418.
[5] J.M. Scholtz, S. Marqusee, R.L. Baldwin, E.J. York, J.M. Stewart, M. Santoro, D.W. Bolen, Calorimetric determination of the enthalpy change for the alpha-helix to coil transition of an alanine peptide in water, Proc. Natl. Acad. Sci. U S A. 88 (1991) 2854–2858.
[6] L. Serrano, J. Sancho, M. Hirshberg, A.R. Fersht, Alpha-helix stability in proteins I. Empirical correlations concerning substitution of side-chains at the N and C-caps and the replacement of alanine by glycine or serine at solvent-exposed surfaces, J. Mol. Biol. 227 (1992) 544–559.
[7] M. Lopez de la Paz, E. Lacroix, M. Ramirez-Alvarado, L. Serrano, Computer-aided design of beta-sheet peptides, J. Mol. Biol. 312 (2001) 229–246.
[8] M. Ramirez-Alvarado, T. Kortemme, F.J. Blanco, L. Serrano, Beta-hairpin and beta-sheet formation in designed linear peptides, Bioorg. Med. Chem. 7 (1999) 93–103.
[9] C.K. Smith, L. Regan, Guidelines for protein design: the energetics of beta sheet side chain interactions, Science 270 (1995) 980–982.
[10] V. Munoz, R. Ghirlando, F.J. Blanco, G.S. Jas, J. Hofrichter, W.A. Eaton, Folding and aggregation kinetics of a beta-hairpin, Biochemistry 45 (2006) 7023–7035.
[11] W.A. Eaton, V. Munoz, P.A. Thompson, C.K. Chan, J. Hofrichter, Submillisecond kinetics of protein folding, Curr. Opin. Struct. Biol. 7 (1997) 10–14.
[12] A.G. Cochran, N.J. Skelton, M.A. Starovasnik, Tryptophan zippers: stable, monomeric beta -hairpins, Proc. Natl. Acad. Sci. USA 98 (2001) 5578–5583.
[13] A.R. Viguera, L. Serrano, Bergerac-SH3: "frustration" induced by stabilizing the folding nucleus, J. Mol. Biol. 311 (2001) 357–371.
[14] A.R. Viguera, J.C. Martinez, V.V. Filimonov, P.L. Mateo, L. Serrano, Thermodynamic and kinetic analysis of the SH3 domain of spectrin shows a two-state folding transition, Biochemistry 33 (1994) 2142–2150.
[15] W. Kabsch, Automatic processing of rotation diffraction data from crystals of initially unknown symmetry and cell constants, J. Appl. Cryst. 26 (1993) 795–800.
[16] A. Vagin, A. Teplyakov, MOLREP: an Automated Program for Molecular Replacement, J. Appl. Cryst. 30 (1997) 1022–1025.
[17] J.C. Martinez, M.T. Pisabarro, L. Serrano, Obligatory steps in protein folding and the conformational diversity of the transition state, Nat. Struct. Biol. 5 (1998) 721–729.
[18] P. Emsley, K. Cowtan, Coot: model-building tools for molecular graphics, Acta Crystallogr. D Biol. Crystallogr. 60 (2004) 2126–2132.
[19] G.N. Murshudov, A.A. Vagin, E.J. Dodson, Refinement of macromolecular structures by the maximum-likelihood method, Acta Crystallogr. D Biol. Crystallogr. 53 (1997) 240–255.
[20] O.V. Tsodikov, M.T. Record, Y.V. Sergeev, Novel computer program for fast exact calculation of accessible and molecular surface areas and average surface curvature, J. Comput. Chem. 23 (2002) 600–609.
[21] A.A. Senin, S.A. Potekhin, E.I. Tiktopulo, V.V. Filimonov, Differential scanning microcalorimeter SCAL-1, J. Therm. Anal. Cal. 62 (2000) 153–160.
[22] J.C. Martinez, V.V. Filimonov, P.L. Mateo, G. Schreiber, A.R. Fersht, A calorimetric study of the thermal stability of barstar and its interaction with barnase, Biochemistry 34 (1995) 5224–5233.
[23] J. Ruiz-Sanz, A. Simoncsits, I. Toro, S. Pongor, P.L. Mateo, V.V. Filimonov, A thermodynamic study of the 434-repressor N-terminal domain and of its covalently linked dimers, Eur. J. Biochem. 263 (1999) 246–253.
[24] V.V. Filimonov, A.I. Azuaga, A.R. Viguera, L. Serrano, P.L. Mateo, A thermodynamic analysis of a family of small globular proteins: SH3 domains, Biophys. Chem. 77 (1999) 195–208.
[25] D. Wildes, L.W. Anderson, A. Sabogal, S. Marqusee, Native state energetics of the Src SH2 domain: evidence for a partially structured state in the denatured ensemble, Protein Sci. 15 (2006) 1769–1779.
[26] D.A. Prokhorov, M.A. Timchenko, Y.A. Kudrevatykh, D.V. Fedyukina, L.V. Gushchina, V.S. Khristoforov, V.V. Filimonov, V.P. Kutyshenko, Study of the structure and dynamics of a chimerical variant of the SH3 domain (SHA-Bergerac) by NMR spectroscopy, RJBC 34 (2008) 645–653.
[27] A.R. Viguera, L. Serrano, Hydrogen-exchange stability analysis of Bergerac-Src homology 3 variants allows the characterization of a folding intermediate in equilibrium, Proc. Natl. Acad. Sci. USA 100 (2003) 5730–5735.
[28] B. Morel, S. Casares, F. Conejero-Lara, A single mutation induces amyloid aggregation in the alpha-spectrin SH3 domain: analysis of the early stages of fibril formation, J. Mol. Biol. 356 (2006) 453–468.
[29] E.S. Cobos, V.V. Filimonov, M.C. Vega, P.L. Mateo, L. Serrano, J.C. Martinez, A thermodynamic and kinetic analysis of the folding pathway of an SH3 domain entropically stabilised by a redesigned hydrophobic core, J. Mol. Biol. 328 (2003) 221–233.
[30] G.I. Makhatadze, P.L. Privalov, Heat capacity of proteins. I. Partial molar heat capacity of individual amino acid residues in aqueous solution: hydration effect, J. Mol. Biol. 213 (1990) 375–384.
[31] T. Lazaridis, M. Karplus, Heat capacity and compactness of denatured proteins, Biophys. Chem. 78 (1999) 207–217.
[32] R.S. Spolar, J.R. Livingstone, M.T. Record Jr., Use of liquid hydrocarbon and amide transfer data to estimate contributions to thermodynamic functions of protein folding from the removal of nonpolar and polar surface from water, Biochemistry 31 (1992) 3947–3955.
[33] T. Ooi, M. Oobatake, G. Nemethy, H.A. Scheraga, Accessible surface areas as a measure of the thermodynamic parameters of hydration of peptides, Proc. Natl. Acad. Sci. USA 84 (1987) 3086–3090.
[34] J.K. Myers, C.N. Pace, J.M. Scholtz, Denaturant m values and heat capacity changes: relation to changes in accessible surface areas of protein unfolding, Protein Sci. 4 (1995) 2138–2148.
[35] J. Gomez, E. Freire, Thermodynamic mapping of the inhibitor site of the aspartic protease endothiapepsin, J. Mol. Biol. 252 (1995) 337–350.
[36] A.L. Cortajarena, G. Lois, E. Sherman, C.S. O'Hern, L. Regan, G. Haran, Non-random-coil behavior as a consequence of extensive PPII structure in the denatured state, J. Mol. Biol. 382 (2008) 203–212.
[37] M.L. Tiffany, S. Krimm, Effect of temperature on the circular dichroism spectra of polypeptides in the extended state, Biopolymers 11 (1972) 2309–2316.
[38] R.W. Woody, Circular dichroism and conformation of unordered polypeptides, Adv. Biophys. Chem. 2 (1992) 37–79.
[39] J.C. Martinez, L. Serrano, The folding transition state between SH3 domains is conformationally restricted and evolutionarily conserved, Nat. Struct. Biol. 6 (1999) 1010–1016.
[40] J.C. Martinez, A.R. Viguera, R. Berisio, M. Wilmanns, P.L. Mateo, V.V. Filimonov, L. Serrano, Thermodynamic analysis of alpha-spectrin SH3 and two of its circular permutants with different loop lengths: discerning the reasons for rapid folding in proteins, Biochemistry 38 (1999) 549–559.

[41] V.V. Filimonov, V.V. Rogov, Reversible association of the equilibrium unfolding intermediate of lambda Cro repressor, J. Mol. Biol. 255 (1996) 767–777.
[42] T. Lazaridis, G. Archontis, M. Karplus, Enthalpic contribution to protein stability: insights from atom-based calculations and statistical mechanics, Adv. Protein Chem. 47 (1995) 231–306.
[43] G.I. Makhatadze, P.L. Privalov, Energetics of protein structure, Adv. Protein Chem. 47 (1995) 307–425.
[44] F. Avbelj, R.L. Baldwin, Role of backbone solvation in determining thermodynamic beta propensities of the amino acids, Proc. Natl. Acad. Sci. USA 99 (2002) 1309–1313.
[45] V.V. Filimonov, S.A. Potekhin, S.V. Matveev, P.L. Privalov, Thermodynamic analysis of scanning microcalorimetry data. 1. Algorithms for deconvolution of heat absorption curves, Mol Biol (Mosk) 16 (1982) 551–562.
[46] S. Casares, M. Sadqi, O. Lopez-Mayorga, F. Conejero-Lara, N.A. van Nuland, Detection and characterization of partially unfolded oligomers of the SH3 domain of alpha-spectrin, Biophys. J. 86 (2004) 2403–2413.
[47] K.V. Kishan, G. Scita, W.T. Wong, P.P. Di Fiore, M.E. Newcomer, The SH3 domain of Eps8 exists as a novel intertwined dimer, Nat. Struct. Biol. 4 (1997) 739–743.